Supplementary Material

Expression, Localization and Functional Activity of the Major Na^+/H^+ Exchange Isoforms Expressed in the Intestinal Cell Line Caco-2BBe

Yan Yu[a] Anna Seidler[a] Kunyan Zhou[a] Zhenglin Yuan[a] Sunil Yeruva[a]
Mahdi Amiri[a] Chris C. Yun[b] Katerina Nikolovska[a] Ursula Seidler[a]

[a]Department of Gastroenterology, Hannover Medical School, Hannover, Germany, [b]Division of Digestive Diseases, Department of Medicine, Emory University, Atlanta, GA, USA

Supplementary Figures:

Supplementary Figure 1: mRNA expression for NHE1-3 in Caco-2BBe cells after shRNA-mediated NHE2 silencing (C2NHE2KD cells) in comparison to the scrambled RNA-transfected control cells. The cells were harvested from the culture flasks at 80% confluence. The NHE1 mRNA expression in C2PLK0.1 cells was set to 100%. n=3 flasks from 3 different passages. NHE2 mRNA expression was decreased by ~ 80%.

Supplementary Figure 2: Detection of the VSVG-tagged NHE3 by Western analysis, in the stably transfected C2hNHE3-VSVG cells, and after 5 successive acid suicide selection cycles, which selects cells with high NHE activity. The method was established to select stably NHE-transfected PS120 cells (which do not possess a functional NHE) by strong intracellular acidification in a Na^+-free medium followed by providing a medium with a low Na^+ sodium concentration that allows the high NHE expressers to get rid of their intracellular acid load and survive, also enhances the expression of the hNHE3-VSVG transgene in Caco-2BBe cells, although these cells possess also other NHEs and survive the acid suicide selection cycles at a much higher percentage than PS120 cells.

Supplementary Figure 3: Schematic diagram of the perfusion chamber for separate apical and basolateral perfusion of the filter-grown Caco-2BBe cells. The apical membranes face the objective, and the filter is shown in red. The dimensions of the perfusion channel are 7 mm x 2 mm x 2 mm.

Supplementary Figure 4: mRNA expression of MCT-1 and acid-activated apical Na^+/H^+ exchange after inhibition of MCT-1 in C2PLKO.1 and C2NHE2KD cells differentiated cells. (A) mRNA expression of MCT-1 in differentiated C2PLKO.1 (●) and C2NHE2KD (○) cells using β-actin as control gene. (n=5-6, mean ± SEM). Acid-activated apical Na^+/H^+ exchange after MCT-1 inhibition with AZD3965 in differentiated cells was performed as described in Figure 6 and 9. Cells were pre-treated overnight with 500 nM of AZD3965 and the inhibitor was added 5 minutes before pH_i recovery. pH_i-curve of (B) C2PLKO.1 and (C) C2NHE2KD in the presence of 500 nM AZD3965, (D) comparisons of acid-induced pH_i recovery rates in control and 500 nM AZD3965 treated C2PLKO.1 (●) and C2NHE2KD (○) cells. Inhibition of MCT-1 did not alter the apical Na^+/H^+ exchange rate regardless of the cell genotype. (n=3-4, mean ± SEM).

Supplementary Figure 5: mRNA expression of CFTR and SLC26A3 in 3 days (sub-confluent) and 14 day-differentiated (confluent) filter-grown C2PLKO.1 and C2NHE2KD cells. Comparisons of (A) CFTR and (B) SLC26A3mRNA expression levels between C2PLKO.1 and C2NHE2KD cells using β-actin as control gene. Significant reduction of CFTR, but increase of DRA was detected as the cells proceed from non-differentiated (sub-confluent) to differentiated (confluent) state. (n=3-6, mean ± SEM, n=3-6, mean ± SEM, one-way ANOVA with Tukey's multiple comparison tests, **$p<0.001$). This reciprocal regulation of CFTR and absorptive transporters in the self-differentiating Caco2BBe cell line has already been observed in the lab of Eugene Chang in the early 1990´s and discriminates this

cell lines from that of others, who find an upregulation of CFTR expression with differentiation.

Supplementary Figures:

Supplementary Figure 1

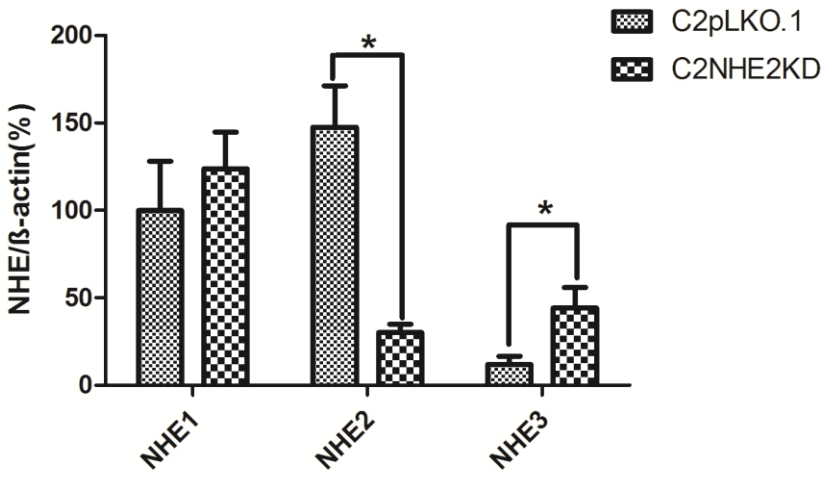

Supplementary Figure 2

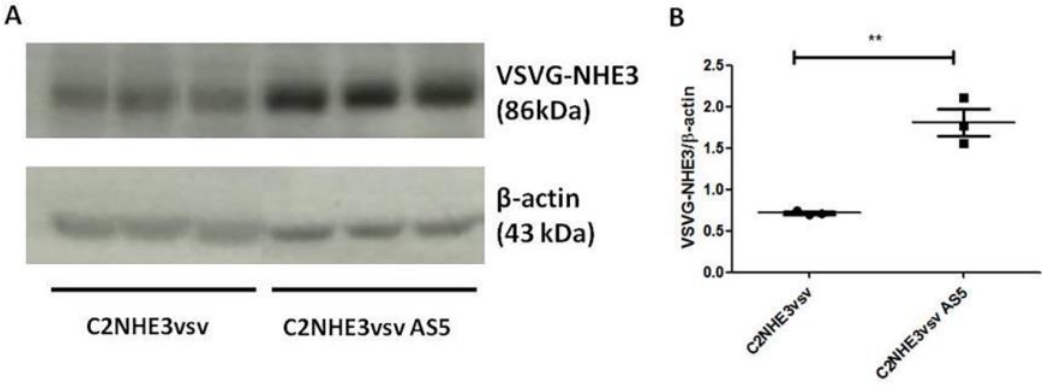

Supplementary Figure 3

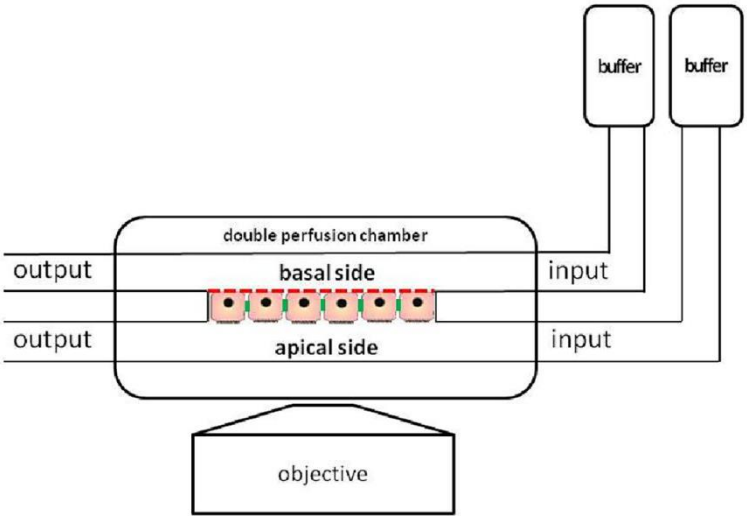

Supplementary Figure 4

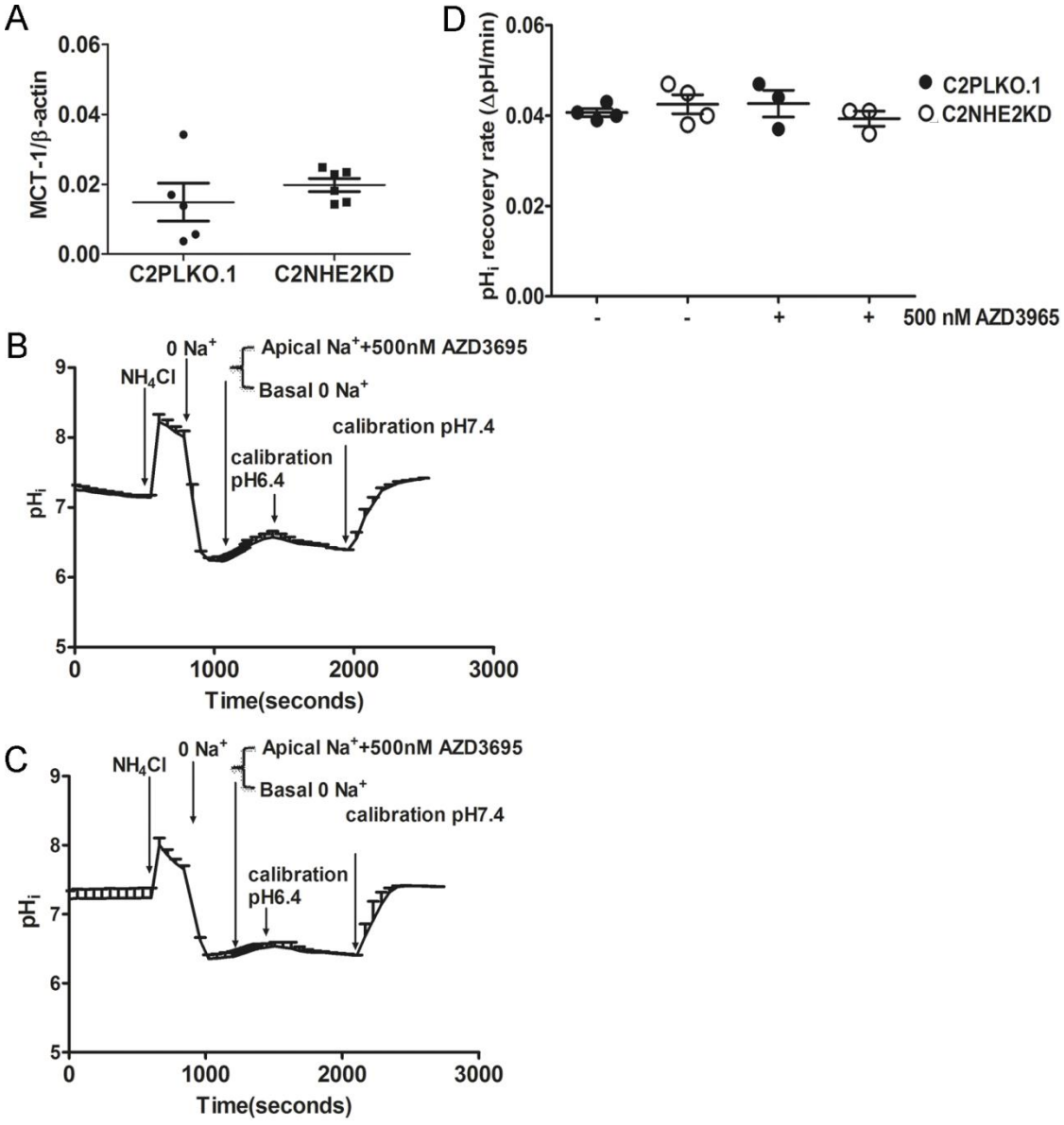

Supplementary Figure 5

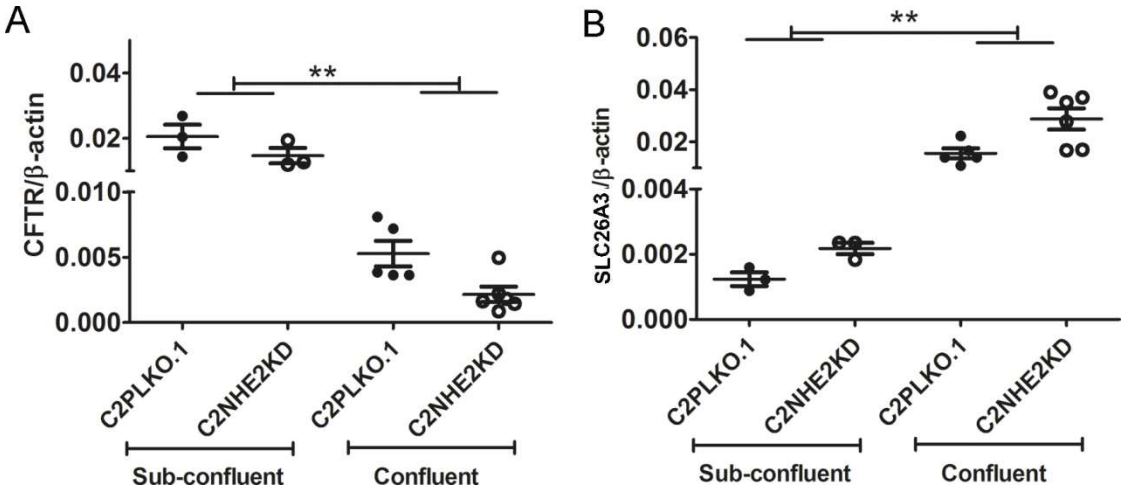

Supplement Table 1: List of primers used for quantitative RT-PCR.

	sequence (5' → 3')	concentration	efficiency
human NHE1	for: GCTGGTGGCAGACCCCTACGA	150 nM	1.946
	rev: ATAGGCCAGTGGGTCTGAGCCGA		
human NHE2	for: CTTCCACTTCAACCTCCCGAT	500 nM	1.904
	rev: GCTGCTATTGCCATCTGCAA		
human NHE3	for: ACCGTGCGCTACACCATGAAGATG	100 nM	1.915
	rev: ATGCGGTAGCGGTTCAGAAGCC		
human NHE8	for: ATGTCAGTGGGTGGCAACA	250 nM	1.877
	rev: ATGGCCATCATGCCTGAGAG		
human Villin	for: CTATGCCAACACCAAGAGAC	500 nM	1.857
	rev: CCCAGACATCTAGTAGGAACAC		
human β-actin	for: CTGGCACCCAGCACAATG	500 nM	1.956
	rev: CCGATCCACACGGAGTACTTG		
human MCT-1	for:CTGTAACACCGTACAGCAACTA	500 nM	1.984
	rev:TGGTCGCCTCTTGTAGAAATAC		
human SLC4A4	for:CCGGCTTTGTTGGTCACTAT	500 nM	2.022
	rev:CAAGTGATACCCTGCTCCTTTC		
human SLC4A7	for:CTGCTATTCCTGCTTTGCTTTG	500 nM	1.869
	rev:GTGATAGCCAGCTCCTTTCTT		
human SLC4A10	for:AGGTTGTCTCCAGCTGTATTG	500 nM	1.978
	rev:TCATGGTACTGTTGACCCTTTC		
human SLC26A3	for:TTCAGTTGCCAGCGTCTATTC	500 nM	1.764
	rev:GTGTTTTGCCTCCTGTGCTCT		
human CFTR	for:TTAGGAGCTTGAGCCCAGAC	500 nM	1.852
	rev:GTCTGACAATTCCAGGCGCT		

Supplement Table 2: Composition of buffers used for pH_i-fluorometry. All concentrations shown are in mM.

	Buffer A (pH7.4)	Buffer B (pH7.4)	Buffer C (pH7.4)	Buffer D (pH6.5)	Buffer E (pH7.35)
NaCl	140			20	20
KCl	1.5	1.5	1.5	21.5	21.5
K_2HPO_4	1.5	1.5	1.5	1.5	1.5
KH_2PO_4	0.5	0.5	0.5	0.5	0.5
$MgSO_4$	1	1	1	1	1
K-Gluconate	1.5	1.5	1.5	100	100
HEPES	10	10	10	10	10
D(+)-Glucose	10	10	10	10	10
NH_4Cl		50			
TMA-Cl		90	140		
nigericin				0.01	0.01